Research Article GU J Sci, Part A, 10(4): 524-541 (2023) 10.54287/gujsa.1357247

Gazi University
Journal of Science
PART A: ENGINEERING AND INNOVATION
http://dergipark.org.tr/gujsa

Investigation of Turkey's Climate for Service Lifetime of Photovoltaic Modules: A Mapping Approach

Abdulkerim GOK[1*]

[1] Department of Materials Science and Engineering, Gebze Technical University, Gebze, Kocaeli, Türkiye

Keywords

PV Modules
Standard Testing
Degradation
Reliability
Service Lifetime

Abstract

The longevity of photovoltaic systems during real-world operation is a concern that needs to be addressed. Polymeric materials used in module constructions, particularly encapsulants, are susceptible to hydrolysis, which can lead to cell metallization corrosion and result in power loss and shortened service lifetime. One of the test protocols within the current certification standard of IEC 61215 is damp heat exposure, which subjects the modules to constant temperature and humidity level for a specific duration (85°C/85%RH for 1000 hours). However, its effectiveness as a reliability test for long-term durability is often debated. This study applies a methodology for calculating the equivalent damp heat testing time that corresponds to a targeted service lifetime (i.e., 30 years) in real-world conditions. The results are presented in the form of a country map, focusing on Turkey, illustrating the variations in testing times across different regions due to local climate conditions. This study shows that applying a single set of conditions for a fixed duration, as applied in the damp heat testing, to all modules with different components and for all climate conditions poses substantial risks when it comes to predicting service lifetime.

Cite

Gok, A. (2023). Investigation of Turkey's Climate for Service Lifetime of Photovoltaic Modules: A Mapping Approach. *GU J Sci, Part A, 10*(4), 524-541. doi:10.54287/gujsa.1357247

Author ID (ORCID Number)

0000-0003-3433-7106 Abdulkerim GOK

Article Process

Submission Date 08.09.2023
Revision Date 06.12.2023
Accepted Date 26.12.2023
Published Date 31.12.2023

1. INTRODUCTION

Over the past decade, the installation of photovoltaic (PV) systems has experienced tremendous growth. The improved cell/module efficiencies and the reduction in manufacturing and electricity generation costs have been the key factors for this robust adoption of PV systems (IEA PVPS, 2022). While the global cumulative capacity of installed PV systems has reached 1.2 TW at the end of 2022, it stands around 9.5 GW in Turkey (IEA PVPS, 2023). However, to ensure sustainable growth, it is crucial to enhance the durability and reliability of PV modules to extend their service lifetime. In the current market, a 30-year power performance warranty is provided for PV modules which guarantees a maximum of 20% power loss by the end of the warranty period. The challenge lies in the fact that this warranty applies universally to all PV modules irrespective of the diverse climate conditions they are installed in. In real-world, PV modules are subjected to a range of environmental stress factors such as heat, humidity, ultraviolet light, and mechanical stresses. Therefore, these varying conditions necessitate the selection of appropriate materials and material combinations for module lamination to enhance the PV modules' durability and reliability. Recent studies not only focus on understanding the degradation mechanisms and failure modes in the currently installed PV modules and systems (Gok et al., 2019; Aghaei et al., 2022), but also search for alternative materials and lamination strategies for improved service lifetime (López-Escalante et al., 2018; Oreski et al., 2020; Adothu et al., 2021). In economic and environmental terms, extending service lifetime will lead to reduced levelized cost of electricity and greenhouse gas emissions for a more sustainable future.

*Corresponding Author, e-mail: agok@gtu.edu.tr

A conventional crystalline silicon (c-Si) PV module, as shown in Figure 1 (GSES, 2023), is constructed using a tempered front glass, solar cells with metallization elements embedded in two layers of encapsulant polymers, a polymeric multi-layer backsheet, a junction box, and an aluminum frame. Encapsulant and backsheet films are known as the packaging polymers that play a crucial role in providing electrical insulation, environmental protection, and mechanical stability to the cells and cell metallization. The most commonly used encapsulant material is ethylene-vinyl acetate (EVA), but it is susceptible to hydrolytic degradation (Oreski et al., 2019), leading to discoloration, delamination, and the corrosion of cell metallization, ultimately reducing the power performance and service lifetime of PV modules.

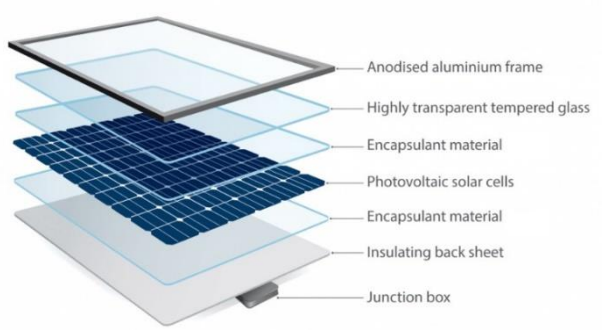

Figure 1. *PV module components*

The IEC 61215 standard (IEC, 2021) for design qualification and type approval for terrestrial PV modules lays down requirements for long-term operation in open-air climates. According to the standard, "the useful service lifetime of modules so qualified will depend on their design, their environment, and the conditions under which they are operated". While it helps identify the premature failures that might occur in the field due to design, processing, and manufacturing flaws, it should not be solely relied upon as a reliability test for estimating service lifetime as explicitly stated by the standard. This standard includes a damp heat exposure protocol to assess the long-term effects of humidity ingress into the module construction. As part of this protocol, PV modules are exposed to a constant temperature of 85°C and a relative humidity level of 85% for 1000 hours. However, passing this test under certain criteria is often mistakenly interpreted as an indication of service lifetime. Given the complexities of the real-world conditions and differences in module constructions, the standard's ability to accurately predict long-term performance has become a topic of intense debate within the PV community (Weiß et al., 2022).

The effect of heat and humidity is one of the most important stressor factors for PV modules in real-world conditions. They particularly contribute to the decline in power performance due to the degradation of polymeric encapsulant materials and corrosion of the cell metallization. Even though the damp heat conditions, especially the level of applied temperature, are criticized, a translation of real-world conditions into the laboratory-based testing conditions, or vice versa, is required in order to achieve a successful service lifetime estimation. Koehl et al. (2012, 2017) have proposed a methodology that enables the calculation of equivalent damp heat testing time needed to achieve a targeted service lifetime, taking the activation energy of power degradation caused by humidity-driven reactions during damp heat testing into account. Using the same methodology, this study aims to calculate and map the equivalent damp heat testing times across Turkey in order to examine the variations in climate conditions in different regions and their impact on the corresponding equivalent damp heat testing times. Turkey stands out as one of the unique countries in Europa not only with its gigantic solar energy potential but also with its diverse geographical regions and climate conditions, both of which have tremendous effects on the performance and service lifetime of PV modules.

Like many countries, Turkey is concerned about environmental issues and the impact of conventional energy sources on air quality and climate change. By setting ambitious targets and introducing various regulations and incentives, increasing the share of renewable energy in the total energy mix, including solar PV, is part of the strategy to mitigate these environmental concerns. Recent studies on solar energy research, focusing on Turkey, have mostly deal with solar radiation and energy generation potential forecasts for a specific location (Turan et al., 2023) and, in rare cases, for the entire country (Salmanoğlu & Çetin, 2022), including

performance analysis and economic perspectives of PV systems (Er, 2023). The effect of environmental stress factors on PV system performance and lifetime; however, has been studied either for individual stress factors such as temperature (Çabuk, 2022) or for specific systems and locations (Tirmikçi et al., 2021). Since the installation of PV systems in Turkey has started after the year 2014, there are limited number of experimental and statistical studies dealing with long-term durability and reliability of these systems under real-world conditions.

Instead of specific systems, locations, or stress factors, the mapping approach applied in this study helps us have better insights into the impacts of local climate conditions on the performance of PV systems in the entire country and unveil the risks linked to the application of standard conditions for a certain period of time to all kinds of module constructions and climatic conditions for service lifetime estimation. By considering the specific characteristics of different PV modules and the diverse climatic conditions, this study seeks to contribute to the ongoing discussions within the PV community regarding the accuracy of the existing standard test protocols in determining the long-term performance of PV modules. Although the standard damp heat conditions (85°C and 85%RH) are used, since the analysis workflow is automated, it can be used for the application of different temperature and humidity levels as well.

2. MATERIALS AND METHODS

2.1. Calculation of the Equivalent Damp Heat Testing Times

The analysis process for the calculation of equivalent damp heat testing time for a given location, as outlined by Koehl et al. (2012, 2017), involves the following steps:

1. Calculating the module temperature using the well-known Faiman Model (Faiman, 2008) according to Equation 1 as follows:

$$T_{mod} = T_{amb} + \frac{G_{POA}}{U_0 + U_1 \cdot WS} \tag{1}$$

where T_{amb} and T_{mod} are the ambient and module temperatures (°C), respectively, G_{POA} is the plane or array irradiance (W/m^2), U_0 is the constant heat transfer coefficient (25 W/m^{2}K), U_1 is the convective heat transfer coefficient (6.84 W/m^{3}sK), and WS is the wind speed (m/s).

2. Calculating the surface relative humidity at the module surface and temperature (referred to as micro-climate) according to Equation 2 as follows:

$$RH(T_{mod}) = RH(T_{amb}) \times \frac{p_{sat}(T_{amb})}{p_{sat}(T_{mod})} \tag{2}$$

where $RH(T_{amb})$ and $RH(T_{mod})$ are the surface relative humidity (%) values at the ambient and module temperatures, respectively, and $p_{sat}(T_{amb})$ and $p_{sat}(T_{mod})$ are the water vapor saturation pressures at the ambient and module temperatures, respectively. Water vapor saturation pressure values can be calculated according to Equation 3 as follows:

$$p_{sat} = 10^{0.66077+7.5\times\frac{T}{237.3+T}} \tag{3}$$

where T is either the ambient temperature (°C) for $p_{sat}(T_{amb})$ or the module temperature (°C) for $p_{sat}(T_{mod})$.

3. Calculating the effective surface relative humidity at the module surface and temperature (referred to as sigmoidal model) according to Equation 4 as follows:

$$RH_{eff} = \frac{1}{\left[1 + 98 \times \exp\left(-9.4 \cdot RH(T_{mod})\right)\right]} \tag{4}$$

Koehl et al. (2012, 2017) showed that the sigmoidal model was the best model to represent the impact of the effective surface humidity of PV modules on degradation processes. In this model expression, the factor of 9.4 is a free parameter in the predicted model fitted to the experimental observed test data.

4. Calculating the time periods (Δt_{85}) corresponding to 85% relative humidity as a function of the module temperature according to Equation 5 as follows:

$$\Delta t_{85}(85\%RH, T_{mod}) = \Delta t_{mon} \times \frac{RH_{eff}}{0.85} \tag{5}$$

where Δt_{mon} is the monitored time interval during which the effective relative humidity levels that are assessed are transformed to a contribution of the time period of high relative humidity levels (i.e., here, it is set to 85% relative humidity for the standard testing condition).

5. Applying a time transformation to a constant test temperature and performing integration to calculate the equivalent testing time for a given location required for a specific service lifetime using the Arrhenius relationship according to Equation 6 as follows:

$$\Delta t_{ref} = \sum_{1}^{N} \Delta t_i \cdot \exp\left[\left(-\frac{E_a}{R}\right)\left(\frac{1}{T_i} - \frac{1}{T_{ref}}\right)\right] \tag{6}$$

where Δt_{ref} is the time period in the standard (reference) test conditions, Δt_i is the time interval, E_a is the activation energy of the damp heat driven power degradation processes, which is a free parameter used to investigate the effect of module construction on the equivalent damp heat testing times, T_i is the transient temperature at time intervals of Δt_i, and T_{ref} is the standard (reference) temperature of 85 °C. The calculated testing time (Δt_{ref}) is then multiplied by the number of years anticipated as the service lifetime, i.e., 30 years.

This methodology can be viewed as a means of translating real-world climate conditions into equivalent constant damp heat conditions. When calculating the module temperature, it takes air temperature, irradiance, and wind speed into account, and when calculating the effective surface relative humidity, it treats relative humidity as a dose. As the first step, the analysis workflow assesses the frequency distribution of 85% relative humidity based on module temperature at a given location, and as the second step, it calculates the acceleration factors using the activation energies of power degradation processes. Koehl et al. (2012, 2017) effectively demonstrated this procedure by incorporating four different relative humidity models: (i) ambient relative humidity model accounts for the overall relative humidity in the surrounding environment, (ii) surface relative humidity (or micro-climate) model takes the relative humidity in close proximity to the module surface, acknowledging the influence of the immediate surrounding of the module, and thus, differs from the ambient relative humidity as it is affected by the module temperature, (iii) squared surface relative humidity (or squared micro-climate) model incorporates the hydrolysis kinetics of polymeric materials as some exhibit second-order kinetics with water content, and (iv) effective surface relative humidity (sigmoidal) model represent the sigmoidal shape of the water sorption isotherms of the polymeric encapsulant material, providing more accurate representation of the humidity content in the module construction. By considering these relative models, they conducted the analysis across various selected locations spanning different climate zones. Here, in this study, instead of specific point locations, a more comprehensive approach is applied to produce a country map in order to achieve more thorough understanding of the effects of local climate conditions on the equivalent damp heat testing times and gain more detailed insights into the effect of heat and humidity on different PV module constructions with varying activations energies in different environments.

2.2. Data Preparation

In order to calculate equivalent testing times for precise point locations in Turkey, typical meteorological year (TMY) data were obtained from the Photovoltaic Geographical Information System (PVGIS, 2023) database at a resolution of 0.05 in both latitude and longitude, which corresponds approximately to 5.5 km and 4.3 km in real-scale, respectively. This is the highest resolution provided by the PVGIS database, ensuring accurate spatial representation of the data, aggregating to a total of 43,000 coordinate numbers for Turkey. The TMY

data obtained includes hourly measurements of various meteorological parameters such as global horizontal irradiance (GHI), direct normal irradiance (DNI), diffuse horizontal irradiance (DHI), air pressure, dry-bulb temperature, wind speed and direction, relative humidity, and long-wave downwelling infrared radiation. It provides a comprehensive set of data necessary for the analysis of the climate conditions, however, it is important to note that the data is provided at an hourly resolution, which poses a limitation for the analysis. To address this limitation and ensure robustness, a wider area is covered with closely spaced data points. This approach compensates for the hourly resolution and allows for a more comprehensive assessment.

For each data point, the TMY data was initially retrieved from the PVGIS database and thoroughly examined for any potential corrupt or missing values. Once the data quality is ensured, the processing is carried out in accordance with the aforementioned analysis workflow: (i) evaluation of the frequency distribution of 85% relative humidity as a function of the module temperature, and (2) calculation of the equivalent damp heat testing times for 30 years of service lifetime based on varying activation energies. Since the activation energies for power degradation in PV modules due to humidity driven reactions under the damp heat conditions fall within the range of 0.5 eV to 0.7 eV, as reported in Koehl et al. (2012, 2017), for standard glass/backsheet modules with EVA-based encapsulants, an average activation energy of 0.6 eV is selected for the mapping purposes. The resulting dataset consists of three columns: longitude, latitude, and the corresponding equivalent testing time. It is noteworthy that the computation time for processing the dataset at a resolution of 0.05 was nearly 10 hours without employing any parallelization techniques. This relatively long processing time can be attributed to the size of the dataset, the intricacies of data retrieval, and processing at such high resolution.

2.3. Interpolation Method

The selection of an appropriate interpolation method for mapping requires careful consideration of different approaches and resolutions. Due to the complexity of the task, making the right decision usually needs a lot of experience and specialization in the field, but extensive experimentation with the dataset with various methods and evaluating their performances is usually a reliable strategy. Thus, several interpolation methods and data resolutions are examined, and ultimately, the Inverse Distance Weighting (IDW) method (Watson & Philip, 1985), combined with a dataset resolution of 0.1 in both latitude and longitude, is found to be the most optimal approach in terms of accuracy and computational efficiency. Efficiency is crucial as the study area expands, and time and hardware requirements do not increase linearly.

IDW is a relatively simple interpolation method that assumes a linear relationship between two data points, assigning higher weights to points closer to the target location. This results in a smooth transition of colors in the interpolated map, providing visually appealing and informative representation of data. In comparison, Kriging (Matheron, 1963), another commonly used interpolation method in mapping applications, utilizes a variogram to model the spatial autocorrelation of the data. Nevertheless, the variogram analysis conducted for the dataset indicates a lack of significant spatial autocorrelation, hence rendering Kriging impractical in this study for the mapping process. Furthermore, Kriging exhibits slow computational performance when applied to the dataset of 43,000 data points. Other interpolation methods are also tested, but the results do not significantly differ from IDW, considering the high density and regular arrangement of data points. Therefore, IDW is selected as the appropriate interpolation method due to its ease of use and computational efficiency.

Once the interpolation method is assessed, resolution studies are conducted to optimize the mapping process. It is found that a coordination resolution of 0.1 is sufficient, as it yields similar results compared to a resolution of 0.05, while significantly reducing the data acquisition time, leading to a more efficient mapping process.

2.4. Visualization

For visualization purposes, the dataset of equivalent damp heat testing times is transformed into an informative and visually appealing country map, allowing for a clear representation of the variations across different regions of Turkey. In order to accomplish this task, the following steps are applied using an open-source Geographic Information System (QGIS, 2023) tool: (i) the resulting dataset containing latitude, longitude, and the corresponding equivalent testing time is uploaded into QGIS along with the Turkey's shapefile (EEA, 2023), ensuring that the proper coordinate reference system is used to maintain accurate spatial representation, (ii) the IDW interpolation is applied to the dataset, setting the power constant to four in order to control the

influence of nearby points on the interpolated values and raster sizes of X and Y pixels to 0.05 in order to achieve the desired level of detail in the interpolated map, (iii) the interpolated layer is masked using the shapefile of Turkey, removing any excess parts of the interpolated map that fall outside the boundaries of the country, ensuring that the visualization solely focuses on the relevant area, (iv) the render type is set to single-band pseudo-color to enhance the visualization, allowing for the representation of different values using a color ramp, (v) the interpolation is discretized to provide a more distinct representation of the values, and early resampling techniques are applied to optimize the rendering performance, and (vi) a legend is generated based on the frequency of the values, enabling viewers to interpret the colors in the map.

3. RESULTS AND DISCUSSION

In order to exemplify the analysis workflow for relative humidity frequency profiles in Section 3.1 and equivalent damp heat testing time calculations in Section 3.2, twelve cities located in different geographical regions across the country are selected as examples of location-dependent climate conditions in Turkey. Then, Section 3.3 will follow for the mapping discussion.

3.1. Relative Humidity Frequency Profiles

Figure 2 illustrates the distribution of hours with 85% RH in relation to module temperature considering the four different humidity models for the selected cities. Analyzing diverse geographical regions reveals distinguishable frequency distributions of 85% RH in dry and humid climates, highlighting the importance of the local climate conditions. Significantly higher frequencies are seen in humid climates such as Adana, Antalya, Istanbul, Izmir, Samsun, and Trabzon, and considerably lower frequencies are seen in dry climates such as Ankara, Erzurum, Konya, Sanliurfa, Sivas, and Van. When the ambient temperature, and consequently the module temperature, is low, the humidity levels are high, leading to similar frequency distributions across the different humidity models. On the contrary, as the ambient and module temperatures increase, the humidity levels decrease, resulting in varying frequency distributions among the different humidity models. For hot and humid locations, the peak frequency is observed at the module temperature of around 15°C, but on the other hand, this temperature is around 5°C for mild and dry locations.

3.2. Equivalent Damp Heat Testing Times

Figure 3 illustrates the corresponding equivalent damp heat testing times at 85°C/85%RH for a service lifetime of 30 years as a function of activation energy considering the four different humidity models for the selected cities. It can be noticed that the equivalent damp heat testing times vary tremendously with changing activation energies, highlighting the importance of the module construction. When the activation energy is low, reaction kinetics will be faster, and therefore, the required testing time for the targeted service lifetime will be higher. Similarly, when the activation energy is high, reaction kinetics will be slower, and therefore, the required testing time for the targeted service lifetime will be lower. Regarding the behavior of the different humidity models, a similar conclusion made for the frequency distributions can be drawn here as well. The variation between the models is larger for hot and humid climates, especially at higher activation energies, than that for mild and dry climates.

For further discussion, only the results obtained from the sigmoidal humidity model are presented, as it is established as the most suitable model for estimating the degradation impacts of the effective surface relative humidity on PV module performance.

Table 1 provides the comprehensive list of the equivalent damp heat testing times (in hours) at 85°C/85%RH for a service lifetime of 30 years as a function of activation energy for the effective surface relative humidity (sigmoidal) model for all cities in Turkey. Here, it is to be noted that the official latitude and longitude values of each city are used. Although the calculations are performed for the activation energies of 0.2 eV to 1.4 eV (with 0.1 eV increments), as seen in Figure 3., only the activation energies of 0.3 eV to 0.9 eV are included here due to limited space. As expected, humid climates exhibit higher humidity levels, leading to longer equivalent testing times compared to dry climates. For instance, for an activation energy of 0.6 eV, while only 1268 hours of testing under the damp heat conditions is sufficient to ensure 30 years of lifetime in Sanliurfa (hot and dry climate), 3109 hours of exposure is required for the same lifetime in Adana (hot and humid

climate). The same situation is also true for Van and Izmir. Only 792 hours of testing under the damp heat conditions is adequate to represent 30 years of lifetime in Van (mild and dry climate) for an activation energy of 0.6 eV, whereas Izmir (hot and humid climate) requires 2283 hours of testing for the same lifetime. It is interesting to see that Istanbul necessities more testing time than Trabzon, i.e., 2686 hours for the former and 2153 hours for the latter. Trabzon is known for heavy rainfalls in the country; however, Istanbul has higher humidity content, higher temperature, and higher wind speed conditions than Trabzon. All these factors affect module temperature, and hence the effective humidity levels at the module surface, indicating the importance of the type and the magnitude of effective stress factors.

The findings in Table 1 also demonstrate the strong dependence of the equivalent damp heat testing times on the activation energies for power degradation, and thus, the module construction. For instance, in Konya, the city with the highest installed PV capacity due to irradiation conditions, land availability, and dry climate conditions, the testing time is approximately 1112 hours with an activation energy of 0.6 eV (representing a standard glass/backsheet module construction with an EVA-based encapsulant), but this testing time reduces to around 113 hours with an activation energy of 0.9 eV (representing a double glass module construction with impermeable edge-seal for minimal humidity ingress). This discrepancy highlights that the testing time of 1000 hours, as required by the standard, seems to be reasonable for this specific location. It is still inadequate to accurately represent a service lifetime of 30 years for the former scenario and it is quite excessive for the latter scenario, leading to over-aging.

It is important to note that if the targeted service lifetime is extended beyond the current 30-year period, these testing times, reported in Table 1, will need to be adjusted accordingly. A simple conversion procedure suffices for this task: a testing time is divided by 30 in order to obtain the testing time needed for a 1-year period, and then, multiplied by the desired service lifetime, i.e., 40 years. For instance, 1112 hours of testing time for Konya, for a service lifetime of 30 years with an activation energy of 0.6 eV, are brought up to 1483 hours for a service lifetime of 40 years.

Figure 4 depicts how equivalent damp heat testing times are distributed across all cities in Turkey. It is to be noted that only the activation energies of 0.5 eV, 0.6 eV, and 0.7 eV are included in this density plot for visualization purposes. Regardless of the activation energies, all density curves are characterized by a global maximum at lower equivalent testing times, representing the interior regions in the country with lower humidity levels, and a local maximum at higher equivalent testing times, representing the areas close to coastal regions with higher humidity levels. For 0.6 eV, these correspond approximately to 1200 and 2100 hours, respectively. As the activation energy decreases, population density decreases with a broader distribution.

Figure 5 delineates the similarities and the differences between the cities in the form of a dendrogram generated using the hierarchical clustering method. It is one of the most popular and widely used methods to analyze data in which nodes (i.e., cities) are compared with another based on their similarities (i.e., equivalent damp heat testing times). It is an unsupervised machine learning technique that arranges data points into clusters by progressively merging similar clusters together. This creates a tree-like diagram called a dendrogram, capturing data relationships at different levels of detail. The process continues until either all data points are in one cluster (Johnson, 1967). In the dendrogram, there are two main branches: one with small number of cities with higher temperature and humidity levels, and thus higher testing times, representing the coastal regions, and the other with large number of cities with lower humidity levels, representing mostly the interior regions. In the former, Adana seems to be unique with its harsh climate conditions. In the latter, there are two sub-branches: one with cities close to coastal regions with relatively higher humidity levels, and the other with cities mostly located in the central part of the country, away from coastal regions, with relatively lower humidity levels. The dendrogram also presents one obvious and one interesting fact. The obvious fact is that the neighboring cities (or cities within the same geographical regions or in close proximity to each other) are grouped together as they are expected to have very similar climate conditions. The pairs of Istanbul/Kocaeli, Van/Sirnak, Bingol/Tunceli, Edirne/Tekirdag, and Agri/Erzurum can be given as examples. The interesting fact is that there are clusters with cities from different geographical regions (in distant proximity to each other). This is also expected if they have similar climate conditions specifically in terms of temperature and humidity levels. The pairs of Konya/Kars, Igdir/Afyonkarahisar, Bolu/Yozgat, Kutahya/Sanliurfa, and Hatay/Yalova

can be given as examples. This dendrogram is constructed using the data with an activation energy of 0.6 eV; however, similar dendrograms can be obtained with varying activation energies as grouping will not change.

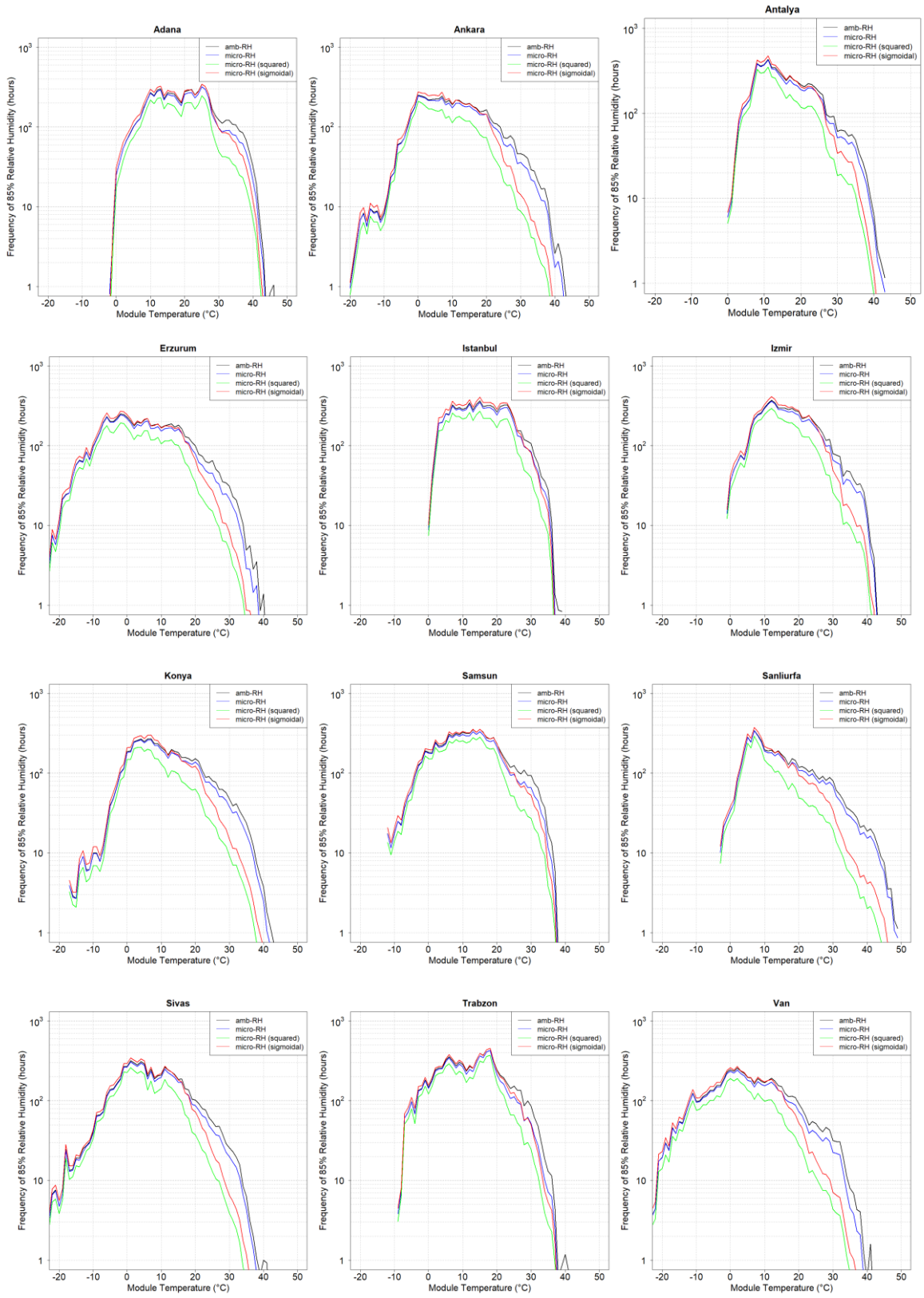

Figure 2. *Frequency distributions of 85% relative humidity in hours as a function of module temperature for the four different humidity models for the selected cities*

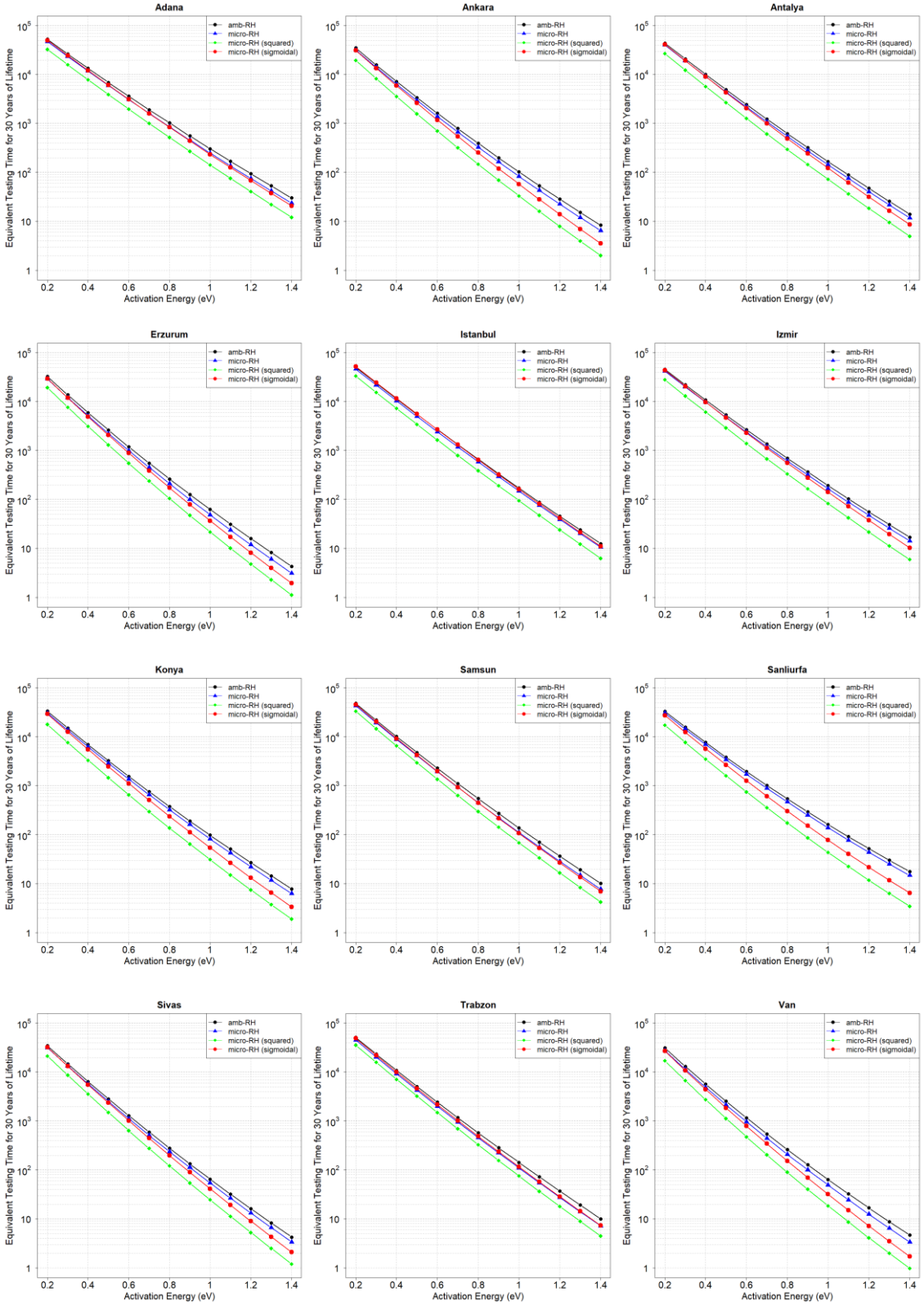

Figure 3. *Equivalent damp heat testing times at 85°C/85%RH for a service lifetime of 30 years as a function of activation energy with the four different humidity models for the selected cities*

Table 1. *Equivalent damp heat testing times at 85°C/85%RH for a service lifetime of 30 years with varying activation energies with the sigmoidal model for all cities in Turkey*

Location	Activation Energy (eV)						
	0.3	0.4	0.5	0.6	0.7	0.8	0.9
Adana	24402.2	12127.6	6103.5	3109.4	1602.8	835.6	440.3
Adiyaman	13655.2	6168.4	2829.1	1317.9	623.7	299.9	146.6
Afyonkarahisar	14206.7	6146.4	2700.9	1205.5	546.5	251.6	117.6
Agri	12329.7	5054.8	2110.8	897.6	388.6	171.2	76.8
Aksaray	11923.8	5201.2	2303.2	1035.8	473.1	219.5	103.5
Amasya	18085.0	8333.5	3898.2	1849.9	890.0	433.8	214.1
Ankara	13455.4	5885.6	2617.0	1182.7	543.1	253.4	120.0
Antalya	19251.3	9039.7	4290.9	2059.4	999.5	490.6	243.5
Ardahan	14581.1	6041.0	2552.4	1098.6	481.3	214.4	97.0
Artvin	18243.2	8270.0	3820.8	1796.7	858.7	416.7	205.0
Aydin	15145.5	6966.2	3247.5	1534.7	735.2	357.1	175.9
Balikesir	19745.3	9222.1	4369.3	2099.1	1022.1	504.1	251.7
Bartin	19709.4	8835.8	4025.7	1863.3	875.6	417.4	201.7
Batman	11434.9	5147.4	2357.3	1099.5	522.8	253.6	125.6
Bayburt	12934.9	5385.0	2286.6	988.9	435.0	194.5	88.2
Bilecik	18528.0	8530.7	3990.0	1894.2	912.0	445.0	219.9
Bingol	12179.3	5131.3	2204.2	964.6	429.6	194.6	89.6
Bitlis	11361.6	4739.6	2012.9	870.5	383.4	172.0	78.5
Bolu	15705.8	6655.6	2869.0	1257.3	559.8	253.0	116.0
Burdur	14199.9	6189.9	2737.4	1228.2	559.0	258.0	120.8
Bursa	19807.6	9072.5	4216.4	1987.1	948.9	458.9	224.6
Canakkale	22211.2	10333.2	4871.7	2326.3	1124.4	549.8	271.8
Cankiri	12774.1	5500.0	2408.4	1072.3	485.3	223.1	104.2
Corum	15478.8	6851.1	3076.4	1401.3	647.2	303.1	143.8
Denizli	13673.8	6308.8	2953.1	1402.8	676.4	331.1	164.5
Diyarbakir	12252.3	5483.9	2498.9	1160.8	550.2	266.4	131.8
Duzce	21622.3	9914.0	4611.0	2174.0	1038.5	502.2	245.8
Edirne	20742.9	9694.9	4581.8	2189.3	1057.6	516.4	254.9
Elazig	12961.2	5702.9	2547.9	1156.2	533.0	249.6	118.7
Erzincan	12434.3	5145.7	2170.4	932.5	407.9	181.5	82.1
Erzurum	11871.1	4894.2	2062.3	887.3	389.3	174.1	79.2
Eskisehir	13782.6	6068.2	2708.2	1225.3	562.1	261.4	123.2
Gaziantep	15714.1	7395.5	3532.8	1712.9	842.8	420.7	213.0
Giresun	16337.7	6812.2	2892.2	1249.4	548.8	244.8	110.9
Gumushane	14034.8	5935.2	2557.3	1121.8	500.6	227.1	104.6
Hakkari	9879.9	3925.6	1590.3	657.0	276.8	118.9	52.1
Hatay	21876.2	10509.6	5105.5	2508.1	1245.8	625.7	317.6
Igdir	13493.2	5916.2	2651.0	1212.3	564.8	267.7	128.9
Isparta	15451.0	6792.4	3026.3	1366.2	624.8	289.4	135.7
Istanbul	24522.0	11611.1	5556.1	2686.2	1311.6	646.6	321.7

Table 1. *(continued)*

Location	Activation Energy (eV)						
	0.3	0.4	0.5	0.6	0.7	0.8	0.9
Izmir	20587.2	9785.4	4701.5	2283.4	1121.1	556.3	279.1
Kahramanmaras	15242.7	6962.9	3228.6	1519.2	725.1	350.9	172.1
Karabuk	18398.2	8249.5	3757.1	1737.3	815.3	388.0	187.1
Karaman	12191.3	5328.0	2360.3	1060.1	482.8	222.9	104.4
Kars	14112.4	5938.9	2549.1	1114.9	496.4	224.8	103.5
Kastamonu	15907.0	6917.3	3055.2	1370.2	623.8	288.1	135.0
Kayseri	12045.9	4996.5	2111.6	909.0	398.3	177.6	80.6
Kirikkale	12294.9	5409.9	2424.8	1107.1	514.8	243.8	117.5
Kirklareli	22328.8	10322.1	4835.6	2294.2	1101.6	535.0	262.6
Kirsehir	12298.8	5359.3	2376.1	1071.6	491.4	229.0	108.4
Kilis	16117.9	7582.4	3616.6	1749.0	857.5	426.2	214.6
Kocaeli	24076.2	11394.1	5468.9	2660.5	1311.0	653.9	330.0
Konya	12651.3	5538.3	2462.6	1112.4	510.5	238.0	112.8
Kutahya	14710.3	6415.3	2840.7	1276.8	582.3	269.4	126.4
Malatya	11643.9	5147.9	2312.7	1055.9	490.1	231.2	110.8
Manisa	16725.2	7616.3	3511.9	1639.6	774.9	370.7	179.5
Mardin	11842.7	5352.6	2461.3	1152.2	549.5	267.1	132.3
Mersin	15822.5	7037.9	3176.8	1454.9	675.8	318.2	151.8
Mugla	19340.2	9129.8	4362.1	2109.7	1032.7	511.7	256.5
Mus	12126.6	5157.4	2235.1	986.7	443.4	202.8	94.3
Nevsehir	14390.8	6361.5	2855.9	1302.2	603.0	283.6	135.4
Nigde	11816.5	4971.8	2130.3	929.1	412.3	186.0	85.3
Ordu	20472.0	9193.5	4195.3	1944.6	915.1	436.9	211.5
Osmaniye	21255.1	10353.0	5113.3	2559.8	1298.4	666.9	346.8
Rize	17427.9	7353.6	3149.9	1369.6	604.3	270.5	122.7
Sakarya	22787.7	10643.2	5041.5	2420.5	1177.2	579.7	288.8
Samsun	20413.7	9241.6	4247.2	1980.6	936.7	449.0	218.0
Siirt	11380.8	4967.4	2206.1	997.7	459.7	216.0	103.5
Sinop	18360.7	8201.6	3722.4	1715.6	802.4	380.6	182.9
Sivas	13205.5	5529.2	2352.4	1016.7	446.2	198.8	89.9
Sanliurfa	12429.8	5709.7	2666.8	1267.6	613.7	302.7	152.2
Sirnak	8893.0	3791.9	1649.6	732.9	332.9	154.7	73.5
Tekirdag	20956.1	9735.9	4583.8	2186.6	1056.4	516.7	255.7
Tokat	16561.7	7261.5	3235.3	1463.6	671.7	312.6	147.4
Trabzon	21998.1	10000.8	4610.4	2153.8	1019.0	488.0	236.3
Tunceli	11978.6	5065.8	2187.0	963.4	432.8	198.2	92.5
Usak	12728.8	5614.3	2514.1	1143.2	527.9	247.5	117.9
Van	10788.1	4422.9	1852.4	792.0	345.4	153.6	69.6
Yalova	23066.5	10892.5	5209.3	2522.3	1235.9	612.6	307.0
Yozgat	14288.9	6255.9	2783.1	1257.7	577.1	268.8	127.0
Zonguldak	22312.9	10295.2	4820.1	2288.9	1101.7	537.3	265.3

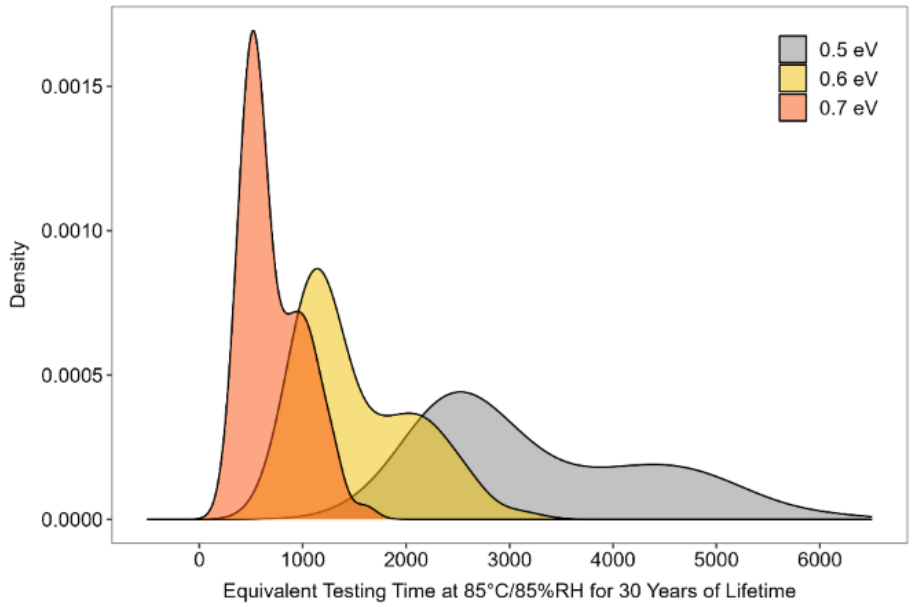

Figure 4. *Distribution of equivalent damp heat testing times at 85°C/85%RH for a service lifetime of 30 years with varying activation energies with the sigmoidal model all cities in Turkey*

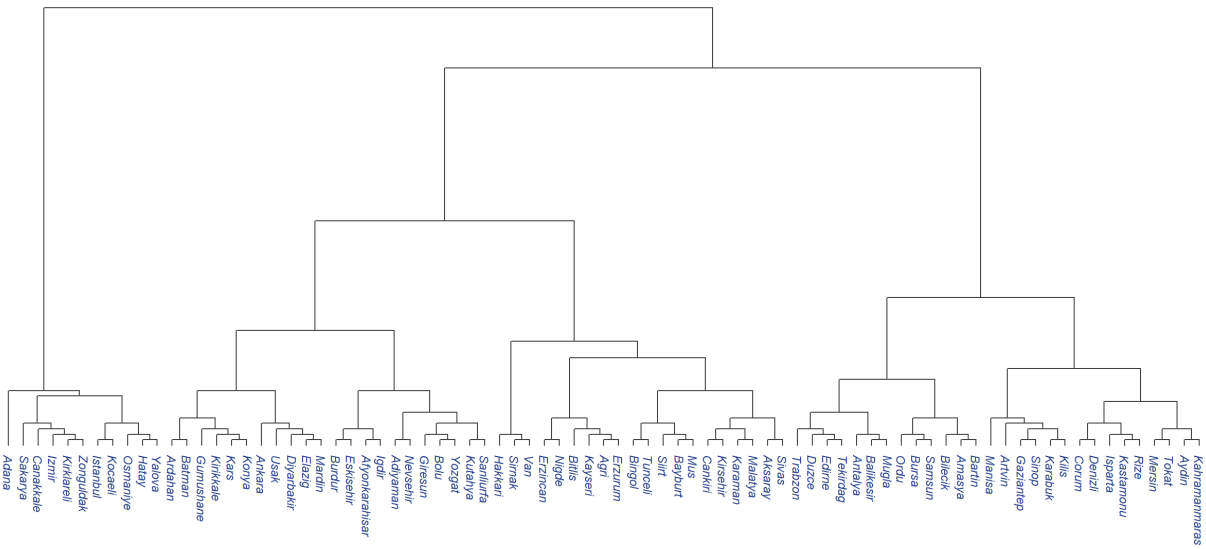

Figure 5. *Hierarchical clustering dendrogram of cities in Turkey, showing their similarities in terms of equivalent damp heat testing times*

3.3. Equivalent Damp Heat Testing Time Map of Turkey

Since the degradation of power in typical glass/backsheet PV modules with EVA-based encapsulants, caused by hydrolytic reactions under the damp heat conditions, exhibits activation energies ranging from 0.5 eV to 0.7 eV, an average activation energy of 0.6 eV is applied for the visualization purposes in mapping procedure. Figure 6 illustrates the map of Turkey, displaying the equivalent testing times required under the standard damp heat conditions (at 85°C/85%RH) for a service lifetime of 30 years generated by using the sigmoidal model for the effective surface relative humidity with an activation energy of 0.6 eV for power degradation. The coastal areas, characterized by higher relative humidity levels, with hot and humid climate conditions, necessitate longer testing times to achieve the desired service lifetime compared to the interior regions with mild/hot and dry climate conditions. This is particularly notable in the Southern, Western, and Northwestern regions. Surprisingly, despite the expectation of longer testing times in the coastal areas of the Northern region, the lower temperature values in this area result in shorter testing times compared to the Southern and Western

coasts. While the central parts show moderate testing times, Eastern and Southeastern regions, as anticipated due to their dry climate conditions, exhibit the shortest testing times in the country.

It is seen that the equivalent testing times exhibit a strong dependence on the location, given the significant variations in local climate conditions, specifically temperature and relative humidity, even within this relatively small country. Best places for PV installations seem to be the Southern-Central, Southeastern-Central, Eastern, and Southeastern regions, characterized by blue areas, followed by mostly interior regions, that are away from the coasts with high humidity content, characterized by the green areas. However, in order for this observation to be completely true, additional factors, such as the irradiation conditions, must be considered. Irradiation condition is, of course, the most important factor for modules to produce electricity. Terrain information is also essential because lands to be used for PV systems, particularly for utility scales, should be feasible for installation, for which urban/residential areas, forests, crop fields, etc., are out of option.

While the current study focuses on providing a country-specific map, our future endeavors encompass a more comprehensive approach. We aim to generate a worldwide map that takes varying activation energies associated with different module constructions and desired service lifetimes into account. By expanding our scope, we aspire to provide a broader understanding of the intricate relationship between module construction, climatic conditions, and the necessary testing durations for PV modules on a global scale. Multi-level maps, combining climatic conditions, irradiation conditions, and terrain information, should also be generated for a more complete understanding of the trade-offs between the performance, reliability, and service lifetime issues.

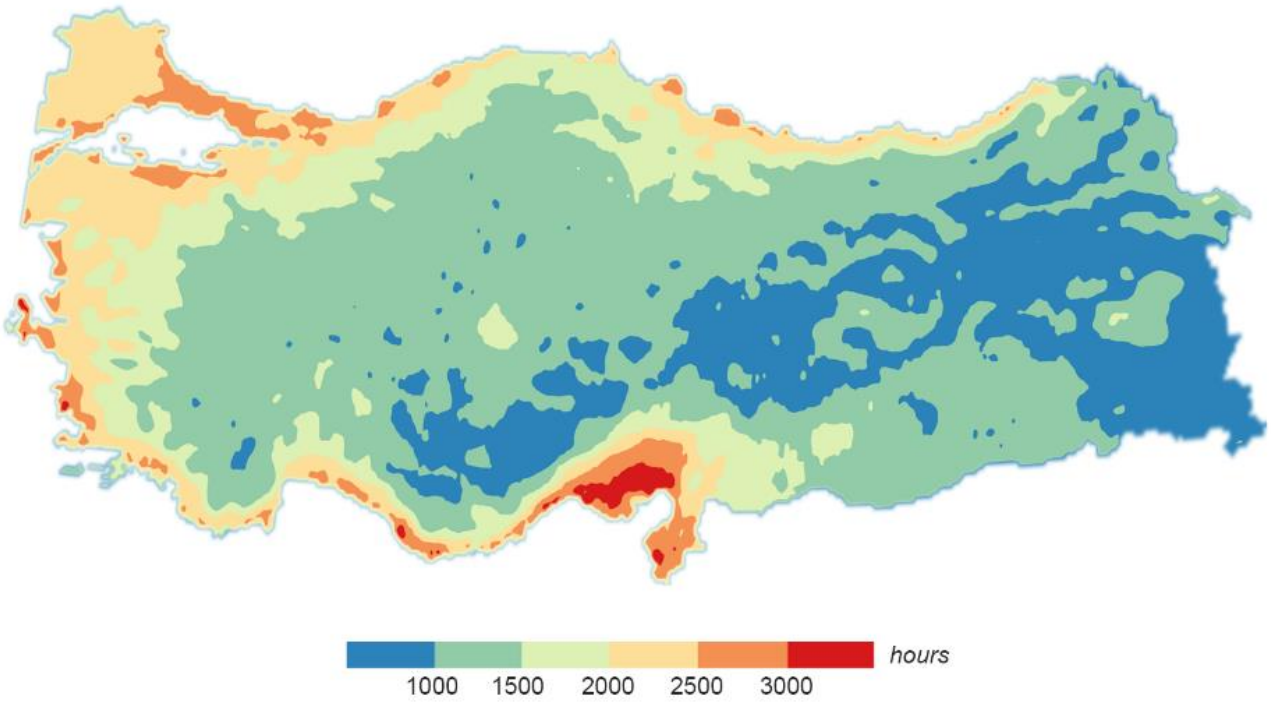

Figure 6. *Equivalent damp heat testing times map of Turkey for a service lifetime of 30 years with an activation energy of 0.6 eV for the effective surface relative humidity (sigmoidal) model*

3.4. The Drawbacks of Standard Testing for Service Lifetime Prediction

Lab-based standard accelerated testing usually involves single and/or constant stress factors applied at elevated intensity levels for a relatively short time frames (compared to the expected service lifetime in real-world operation). Three testing protocols, concerning the durability of module packaging materials and laminated structure, in the IEC 61215 standard, are worth mentioning. Damp heat testing, which is the main focus of this study, is applied to determine the ability of the module construction to withstand the effects of long-term penetration of humidity. In this protocol, temperature and humidity levels are kept constant at 85°C and 85%RH for 1000 hours. Thermal cycling (TC200) testing, on the other hand, is applied to determine the ability of the module construction to withstand thermal mismatch, fatigue and other stresses caused by repeated

changes of temperature. In this protocol, modules are subjected to thermal cycles between -40°C and 85°C (with no humidity content) for 200 times. Similarly, humidity-freeze (HF10) testing is applied to determine the ability of the module construction to withstand the effects of high temperature and humidity followed by sub-zero temperatures. In this protocol, modules are subjected to thermal cycles between -40°C (with no humidity control) and 85°C (with 85% humidity content) for 10 cycles. In the latter two protocols that involve thermal cycles, maximum cycle times, minimum dwell times at each temperature level, and the heating and cooling rates are specified by the standard. There also exist protocols for testing mechanical stability, such as static mechanical load test to determine the ability of the module construction to withstand wind, snow, static or ice loads, and hail test (as a dynamic mechanical impact test) to verify that the module construction is capable of withstanding the impact of hailstones. Other than the protocols for determining characteristic module parameters, the standard also consists of test protocols to investigate the other aspects of failures, mostly related to safety and performance of electrical components, such as insulation test, wet leakage current test, robustness of terminations, hot-spot endurance test, and bypass diode thermal test. Procedures for each testing and requirements for qualification are determined by the standard.

The primary purpose of standard testing for PV modules is to assess the overall construction integrity for design approval and qualification. While it is effective in identifying design and processing flaws that could lead to early failures and safety issues in the field, with its pass/fail nature lacking experimental depth, it offers limited insight into module behavior over the intended service lifetime of 30 years in real-world conditions. Unlike standard testing, which uses single or constant stress factors, actual PV module operation involves multiple, uncontrolled, and cyclic stress factors acting simultaneously with varying intensities during real-world operation. Fielded modules often exhibit various concurrent degradation mechanisms (IEA PVPS, 2014) due to interactions among different stress factors, resulting in complex degradation pathways. The overall degradation or performance loss in this case depends on the integrated effects of all stress factors. Standard testing, accelerated for quick observations, only assesses how modules perform under specific stress conditions and fails to consider the diverse degradation mechanisms active throughout the lifetime. Owing to its simplicity, cost-effectiveness, and shorter test durations, standard testing is preferred over real-world testing to assure reliability for market introduction. Osterwald and McMahon (2009) emphasize that despite aspirations, the conventional standards are not designed as service lifetime tests and argue that establishing a universal test or series of tests for service lifetime prediction of any arbitrary module for 30 years would be impractical. Of course, as they state, this challenge is not unique to the field of PV as various other industries dealing with durable, high-value products, that are expected to maintain long-term performance, like building materials, confront comparable issues. Therefore, there is a growing debate within the PV community about the standard’s effectiveness to be used as an indicator of service lifetime. Predicting a service lifetime of 30 years based on lab-based exposures may seem practical and advantageous, but it carries risks due to intensified and more aggressive stress levels that can overstress modules and thus trigger unrealistic degradation mechanisms that cannot be observed in the field instead of initializing and stimulating realistic ones to a greater extent. Manufacturers may take unnecessary measures to meet stringent requirements solely to pass standards without improving performance of modules in real-world. The study by Jordan et al. (2017) reveals the impacts of climate and module construction on the observed field failures with a comprehensive survey of older and newer installations. They reported that (1) modules installed in hot and humid climates exhibited a broader range of degradation mechanisms compared to those other climates, (2) delamination and diode/junction-box problems were also more prevalent in hot and humid climates, (3) encapsulant discoloration emerged as the most common degradation mechanisms especially in older systems, and (4) newer modules primarily suffered from hot spots, followed by discoloration in internal circuitry. The debate about the usefulness of standard testing for predicting service lifetime therefore revolves mainly around the complexity of real-world conditions, diverse module constructions, and various mounting configurations. While some of the current installations might share similarities with their designs and bill-of-materials that have been in use for maybe 20+ years, considering the history of commercial installations, many of today's modules have distinct differences, probably using lower cost components, from those with a documented history. On that account, it is uncertain whether modules installed today will continue to operate effectively for 30 years.

Numerous studies in the literature have also unveiled the drawbacks associated with utilizing damp heat testing as a predictor for the service lifetime of modules and module materials. For instance, Pickett (2015) investigated the degradation behavior of polyethylene terephthalate (PET) and polycarbonate (PC) polymers

under the standard damp heat conditions of 85°C and 85%RH. Although PET degraded more quickly than PC under these conditions, extrapolating the results to an ambient temperature of 25°C using the Arrhenius relationship revealed that PET outlasted PC due to their distinct activation energies. Both polymers exceeded the standard required lifetime by a significant margin. Similarly, Kempe and Wohlgemuth (2013) explored the hydrolysis kinetics of PET used in PV backsheets, finding that 1000 hours of damp heat testing equated to 150 years of real-world exposure in Bangkok, Thailand. This location is known for its very harsh climate conditions for PV modules with very high levels of temperature and humidity content, suggesting that testing time could be extended to thousands of years in milder climates. Using micro-climate data and finite elements analysis, Hülsmann and Weiss (2015) found that humidity content in the encapsulant polymer between the cells and front glass, induced by damp heat testing, was twice as high as real-world weathering over 20 years. Similarly, Reisner et al. (2006) determined that 1000 hours of damp heat was equivalent to only 16 years in a tropical climate, but to over 100 years in a moderate climate, for the degradation of polyurethane-type encapsulant material in rear-insulated PV modules which usually run 25°C hotter than free-standing modules in mild climates. The correlation between damp heat testing and real-world exposure was found to be inconsistent in the study by Whitfield et al. (2012). They observed higher failure rates under damp heat conditions due to elevated relative humidity content compared to real-world conditions, suggesting a lower overall risk of field failure. After reviewing failures occurred in the field and under damp heat testing, Wohlgemuth and Kempe (2013) asserted that failures driven by field conditions cannot be accurately reproduced by damp heat testing. Additionally, Kempe et al. (2015) explored equivalent damp heat testing times for various module constructions under diverse climate conditions by conducting damp heat testing at various temperature and relative humidity levels and using finite element analysis with real-world meteorological data to predict and compare humidity ingress profiles. For example, 3700 hours of testing (for an open-rack mounted glass/backsheet module with an activation energy of around 0.57 eV) was found to be required to represent a service lifetime of 25 years in a tropical climate. This finding aligns well with the results obtained within this work. Further study by Fan et al. (2018), using empirical kinetics modeling and gamma processes, demonstrated that service life approximations of 20 to 25 years can be achieved under conditions of 50°C/45%RH, underling the severity of the standard damp heat conditions of 85°C/85%RH. Likewise, Kimball et al. (2016) estimated damp heat acceleration factors for a service lifetime of 25 years for over 2500 locations worldwide using empirical kinetics modeling and real-world meteorological data. They concluded that 1000 hours of damp heat adequately represented most locations, even in tropical climates, for humidity-resistant module constructions with an activation energy of around 0.9 eV. Similar to our work, the significant impact of activation energy on testing times was evident in this study as well. On this topic, Laronde et al. (2012) emphasized the need for precise identification of activation energy as a 10% variation in activation energy was shown to alter the estimated service lifetime by 30%.

Warranties for module performance, universally applied to all kinds of modules deployed in all climates, are solely based on established standards. However, findings from this and other studies in the literature clearly indicate that the uncertainty arising from standard damp heat testing results poses a significant challenge in predicting the service lifetime. This is particularly concerning given the intricacies of real-world conditions, diverse module constructions, and varying mounting configurations. To effectively address the reliability issues and improve the performance and service lifetime of PV modules, understanding of degradation mechanisms and failure modes specific to different module types and climate conditions and developing standards that can closely simulate real-world conditions are essential.

4. CONCLUSION

In this study, the analysis of equivalent damp heat testing times to simulate a service lifetime of 30 years for PV modules in Turkey was conducted. With a meticulous approach, the calculations were performed with a resolution of 0.1 in both latitude and longitude values. The obtained results were then presented in the form of a country map, employing an interpolation technique. By mapping, the variations in climatic conditions, and consequently, the effective stress factors were identified, underlining the influence of these factors on the required damp heat testing times necessary to achieve a desired service lifetime for PV modules.

The outcomes of this investigation have shed light on the risks associated with relying solely on standard testing procedures for predicting service lifetime of PV modules across diverse module constructions and

climatic conditions. It has become evident that the durability and reliability of PV modules in real-world scenarios is significantly influenced by both the specific module construction, as it directly affects the kinetics of degradation processes, and the prevailing climatic conditions, as they directly impact the effective stress factors experienced by the PV modules.

As a future work, instead of a country-specific map, a worldwide map to capture the global picture of the service lifetime issues is anticipated. A multi-level mapping, that involves both climate and irradiation conditions, along with the terrain information, to pinpoint the best possible locations for PV system installations for increased performance and reliability can further be persuaded.

ACKNOWLEDGEMENT

This work is conducted as part of the Solar-Era.NET project: PV40+ and supported by the funding from The Scientific and Technological Research Council of Turkey (TUBITAK) under the Grant No: 120N520. The author would like to thank Vahit A. Yenigul for helping with the mapping procedure.

CONFLICT OF INTEREST

The author declares no conflict of interest.

REFERENCES

Adothu, B., Costa, F. R., & Mallick, S. (2021). Damp heat resilient thermoplastic polyolefin encapsulant for photovoltaic module encapsulation. *Solar Energy Materials and Solar Cells*, *224*, 111024. https://www.doi.org/10.1016/j.solmat.2021.111024

Aghaei, M., Fairbrother, A., Gok, A., Ahmad, S., Kazim, S., Lobato, K., Oreski, G., Reinders, A., Schmitz, J., Theelen, M., Yilmaz, P., & Kettle, J. (2022). Review of degradation and failure phenomena in photovoltaic modules. *Renewable and Sustainable Energy Reviews*, *159*, 112160. https://www.doi.org/10.1016/j.rser.2022.112160

Çabuk, A. S. (2022). Comparison of innovative and traditional method for optimizing the efficiency of photovoltaic panels. *International Journal of Energy Applications and Technologies*, *9*(2), 45-49. https://www.doi.org/10.31593/ijeat.1082277

EEA (European Environmental Agency). (2023). Turkey shapefile. (Accessed:27/07/2023) URL

Er, Z. (2023). Solar Radiation Forecasts and a Tiny House PV Off-Grid System. *Avrupa Bilim ve Teknoloji Dergisi*, (47), 7-12. https://www.doi.org/10.31590/ejosat.1234216

Faiman, D. (2008). Assessing the outdoor operating temperature of photovoltaic modules. *Progress in Photovoltaics: Research and Applications*, *16*(4), 307-315. https://www.doi.org/10.1002/pip.813

Fan, J., Qian, Z., & Wang, J. (2018, November 6-8). *Photovoltaic Modules Power Degradation and Lifetime Prediction under Accelerated Damp-heat Conditions Based on Gamma Process*. In: Proceedings of the International Conference on Power System Technology (POWERCON), (pp. 93-100). https://www.doi.org/10.1109/POWERCON.2018.8601560

Gok, A., Gordon, D. A., Wang, M., French, R. H., & Bruckman, L. S. (2019). Degradation Science and Pathways in PV Systems. In: H. Yang, L. S. Bruckman, & R. H. French (Eds.), *Durability and Reliability of Polymers and Other Materials in Photovoltaic Modules* (pp. 47-95). William Andrew Publishing. https://www.doi.org/10.1016/B978-0-12-811545-9.00003-3

GSES (Global Sustainable Energy Solutions). (2023). Recycling Solar Panels. (Accessed:27/07/2023) URL

Hülsmann, P., & Weiss, K.-A. (2015). Simulation of water ingress into PV-modules: IEC-testing versus outdoor exposure. *Solar Energy*, *115*, 347-353. https://www.doi.org/10.1016/j.solener.2015.03.007

IEA PVPS. (2014). Review of Failures of Photovoltaic Modules (No. IEA-PVPS T13-01:2014). International Energy Agency (IEA) Photovoltaic Power Systems Programme (PVPS). (Accessed:27/07/2023) URL

IEA PVPS. (2022). Trends in Photovoltaic Applications 2022 (No. IEA PVPS T1-43:2022). International Energy Agency (IEA). (Accessed:27/07/2023) URL

IEA PVPS. (2023). Snapshot of Global PV Markets 2023 (No. IEA-PVPS T1-44:2023). International Energy Agency (IEA) Photovoltaic Power Systems Programme (PVPS). (Accessed:27/07/2023) URL

IEC (International Electrotechnical Society). (2021). IEC 61215-2:2021: Terrestrial photovoltaic (PV) modules—Design qualification and type approval—Part 2: Test procedures. (Accessed:27/07/2023) URL

Johnson, S. C. (1967). Hierarchical clustering schemes. *Psychometrika*, *32*(3), 241-254. https://www.doi.org/10.1007/BF02289588

Jordan, D. C., Silverman, T. J., Wohlgemuth, J. H., Kurtz, S. R., & VanSant, K. T. (2017). Photovoltaic failure and degradation modes. *Progress in Photovoltaics: Research and Applications*, *25*(4), 318-326. https://www.doi.org/10.1002/pip.2866

Kempe, M. D., Panchagade, D., Reese, M. O., & Dameron, A. A. (2015). Modeling moisture ingress through polyisobutylene-based edge-seals: Polyisobutylene-based edge-seals. *Progress in Photovoltaics: Research and Applications*, *23*(5), 570-581. https://www.doi.org/10.1002/pip.2465

Kempe, M. D., & Wohlgemuth, J. H. (2013, June 16-21). *Evaluation of temperature and humidity on PV module component degradation*. In: Proceedings of the IEEE 39th Photovoltaic Specialists Conference (PVSC), (pp. 0120-0125). https://www.doi.org/10.1109/PVSC.2013.6744112

Kimball, G. M., Yang, S., & Saproo, A. (2016, June 5-10). *Global acceleration factors for damp heat tests of PV modules*. In: Proceedings of the IEEE 43rd Photovoltaic Specialists Conference (PVSC), (pp. 0101-0105). https://www.doi.org/10.1109/PVSC.2016.7749557

Koehl, M., Heck, M., & Wiesmeier, S. (2012). Modelling of conditions for accelerated lifetime testing of Humidity impact on PV-modules based on monitoring of climatic data. *Solar Energy Materials and Solar Cells*, *99*, 282-291. https://www.doi.org/10.1016/j.solmat.2011.12.011

Koehl, M., Hoffmann, S., & Wiesmeier, S. (2017). Evaluation of damp-heat testing of photovoltaic modules. *Progress in Photovoltaics: Research and Applications*, *25*(2), 175-183. https://www.doi.org/10.1002/pip.2842

Laronde, R., Charki, A., & Bigaud, D. (2012). Lifetime Estimation of a Photovoltaic Module Subjected to Corrosion Due to Damp Heat Testing. *Journal of Solar Energy Engineering*, *135*(021010). https://www.doi.org/10.1115/1.4023101

López-Escalante, M. C., Fernández-Rodríguez, M., Caballero, L. J., Martín, F., Gabás, M., & Ramos-Barrado, J. R. (2018). Novel encapsulant architecture on the road to photovoltaic module power output increase. *Applied Energy*, *228*, 1901-1910. https://www.doi.org/10.1016/j.apenergy.2018.07.073

Matheron, G. (1963). Principles of geostatistics. *Economic Geology*, *58*(8), 1246-1266. https://www.doi.org/10.2113/gsecongeo.58.8.1246

Oreski, G., Omazic, A., Eder, G. C., Voronko, Y., Neumaier, L., Mühleisen, W., Hirschl, C., Ujvari, G., Ebner, R., & Edler, M. (2020). Properties and degradation behaviour of polyolefin encapsulants for photovoltaic modules. *Progress in Photovoltaics: Research and Applications*, *28*(12), 1277-1288. https://www.doi.org/10.1002/pip.3323

Oreski, G., Ottersböck, B., & Omazic, A. (2019). Degradation processes and mechanisms of encapsulants. In: H. E. Yang, R. H. French, & L. S. Bruckman (Eds.), *Durability and Reliability of Polymers and Other Materials in Photovoltaic Modules* (pp. 135-152). William Andrew Publishing. https://www.doi.org/10.1016/B978-0-12-811545-9.00006-9

Osterwald, C. R., & McMahon, T. J. (2009). History of accelerated and qualification testing of terrestrial photovoltaic modules: A literature review. *Progress in Photovoltaics: Research and Applications*, *17*(1), 11-33. https://www.doi.org/10.1002/pip.861

Pickett, J. E. (2015). Hydrolysis Kinetics and Lifetime Prediction for Polycarbonate and Polyesters in Solar Energy Applications. In: C. C. White, J. Martin, & J. T. Chapin (Eds.), *Service Life Prediction of Exterior*

Plastics (pp. 41-58). Cham: Springer International Publishing. https://www.doi.org/10.1007/978-3-319-06034-7_3

PVGIS (Photovoltaic Geographical Information System). (2023). (Accessed:27/07/2023) URL

QGIS. (2023). Open Source Geographic Information System (GIS). (Accessed:27/07/2023) URL

Reisner, E. U., Stollwerck, G., Peerlings, H., & Shafiq, F. (2006). Humidity in a Solar Module—Horror Vision or Negligible? 2058-2060. Dresden, Germany.

Salmanoğlu, F., & Çetin, N. S. (2022). An Approach on Developing a Dynamic Wind-Solar Map for Tracking Electricity Production Potential and Energy Harvest. *Gazi University Journal of Science Part A: Engineering and Innovation*, *9*(2), 62-78. https://www.doi.org/10.54287/gujsa.1085005

Tirmikçi, C. A., Yavuz, C., & Gümüş, T. E. (2021). Investigating the Effects of Temperature and Relative Humidity on Performance Ratio of a Grid Connected Photovoltaic System. *Academic Platform - Journal of Engineering and Science*, *9*(3), 427-432. https://www.doi.org/10.21541/apjes.894390

Turan, V., Karakuş, C., & Üstün, İ. (2023). Installation of solar power plant in Adıyaman region and analysis of solar energy potential. *International Journal of Energy Applications and Technologies*, *10*(1), 21-25.

Watson, D. F., & Philip, G. M. (1985). A Refinement of Inverse Distance Weighted Interpolation. *Geoprocessing*, *2*(4), 315-327.

Weiß, K.-A., Klimm, E., & Kaaya, I. (2022). Accelerated aging tests vs field performance of PV modules. *Progress in Energy*, *4*(4), 042009. https://www.doi.org/10.1088/2516-1083/ac890a

Whitfield, K., Salomon, A., Yang, S., & Suez, I. (2012, June 3-8). *Damp heat versus field reliability for crystalline silicon*. In: Proceedings of the 38th IEEE Photovoltaic Specialists Conference, (pp. 001864-001870). https://www.doi.org/10.1109/PVSC.2012.6317957

Wohlgemuth, J. H., & Kempe, M. D. (2013, June 16-21). Equating damp heat testing with field failures of PV modules. In: Proceedings of the IEEE 39th Photovoltaic Specialists Conference (PVSC), (pp. 0126-0131). Tampa, FL, USA: IEEE. https://www.doi.org/10.1109/PVSC.2013.6744113